Optimizing the Open-and Closed-Loop Operations of a Batch Reactor

H. Jazayeri-Rad and M. Shahbaznezhad
Department of Automation and Instrumentation, Petroleum University of Technology, 63431, Ahwaz, Iran
Email: jazayerirad@put.ac.ir

***Abstract*—The purpose of this paper is to optimize the function of a batch reactor operating in open and closed loops. A simultaneous optimization method is employed. This optimization method provides optimal solution at a finite number of points in time. However, the actual batch reactor operation may deteriorate if the computed optimal input is improperly applied to the process. In the open-loop operation, an appropriate wave-shaping method is employed to modify the computed optimal discrete input profile to achieve an improved batch operation while simultaneously guaranteeing the enforcements of the path and end-point constraints. In the closed-loop operation, to improve the disturbance rejection capability of the reactor, two optimizer structures based on the nonlinear model predictive control (*NMPC*) are developed. The first structure is founded on a modified version of a conventional approach which utilizes a variable number of finite elements (*VNFE*). The second optimizer introduced in this paper is a newly developed scheme which is compared against the first approach. This approach makes use of a variable number of collocation points (*VNCP*). Simulation studies, considering both of the fixed batch-time problem (*FBTP*) and minimum batch-time problem (*MBTP*), are presented in this paper.**

***Index Terms*—batch reactor, dynamic optimization, path and end-point constraints, nonlinear model predictive control**

I. Introduction

Batch reactors are broadly used in the manufacturing of fine chemicals and other expensive products. In a batch reactor, there are no feed and output product flows while the reaction is being performed. This is an intrinsically unsteady-state operation where temperatures and concentrations dynamically alter with time.

The dynamic optimization of batch processes in recent years [1]-[8] has become an accepted choice for reducing production costs, enhancing product quality, meeting protection requirements and satisfying environmental regulations. The dynamic optimization problem has path and end-point constraints which result in a complex optimization problem.

A commonly used approach to achieve dynamic optimization is known as the simultaneous optimization [9]. The major feature of the simultaneous optimization technique is the fact that the optimization is performed in the space of discretized inputs and states. Therefore, the dynamic equations and discretized constraints of the system are valid only at a limited number of time instants.

In the open-loop batch operations considered in this work, it has been demonstrated that the shape of the manipulating input, constructed using the computed discrete points of the input trajectory, brings about different process responses.

Because of the lack of process measurements, the open-loop batch operations are extremely influenced by the disturbances and model mismatch. If quick response to a disturbance is required, process measurements are fed back to the system and repeated optimizations are implemented online [10]-[15].This paper introduces a new scheme to improve the disturbance rejection capability of the batch reactors operating in a closed-loop implementation.

In the following section, we describe the process and the modelling steps using the first principles equations. Optimization of batch processes and the simultaneous optimization method are reviewed in Section III. In Section IV, the use of dynamic optimization in open-loop operations is portrayed. In this section, a method is proposed to improve the reactor operation. In Section V, two developed online optimization methods are described. Finally, the results obtained are illustrated in Section VI.

II. Modelling of Batch Reactor

An illustration of the reactor is shown in Fig. 1. In the vessel, strongly exothermic successive reactions are presumed to take place. Component A is consumed by chemical reaction producing the product B. Component B further reacts to the undesired by-product C:

$$A \overset{k_1}{\rightarrow} B \overset{k_2}{\rightarrow} C \quad (1)$$

where k_1 and k_2 are rate constants.

The reactor is equipped with a cooling system, a jacket around the reactor vessel. Aziz and Mujtaba [16] investigated both a simple and a detailed model of this reaction system. The detailed model is considered here.

A chemical process can mathematically be described by mole and energy balances, resulting in a differential-algebraic equation (DAE) system. The mole balances for the constant-volume reactor give:

Manuscript received June 16, 2013; revised August 1, 2013.

doi: 10.12720/joace.2.1.8-19

$$\frac{dC_a}{dt} = -2k_1C_a \quad (2)$$

$$\frac{dC_b}{dt} = k_1C_a - k_2C_b \quad (3)$$

$$\frac{dC_c}{dt} = k_2C_b \quad (4)$$

where C_a, C_b, and C_c are the concentrations of components ($kmolm^{-3}$). The temperature dependency of the rate constants follows the Arrhenius rate law:

$$k_i = k_{i,0}\exp\left(-\frac{E_i}{RT}\right) \quad i = 1,2 \quad (5)$$

where $k_{1,0}$ and $k_{2,0}$ are the pre-exponential constants (4.38×10^4 and 3.94×10^5 h^{-1}, respectively); E_1 and E_2 are the activation energy constants (3.49×10^7 and 4.65×10^7 $J\ kmol^{-1}$, respectively); R is the universal gas constant (8314 $J\ kmol^{-1}\ K^{-1}$); and T is the reactor temperature (K).

The energy balances for the model are:

$$\frac{dT}{dt} = \frac{Q_r - Q_m}{C_pV\rho} \quad (6)$$

$$\frac{dT_m}{dt} = \frac{Q_m - Q_j}{C_{pm}V_m\rho_m} \quad (7)$$

$$\frac{dT_j}{dt} = \frac{F_j}{V_j}\left(T_{j0} - T_j\right) + \frac{Q_j}{C_{pj}V_j\rho_j} \quad (8)$$

$$Q_r = -\Delta H_1(k_1C_aV) - \Delta H_2(k_2C_bV) \quad (9)$$

$$Q_m = U_iA_i(T - T_m) \quad (10)$$

$$Q_j = U_oA_o(T_m - T_j) \quad (11)$$

where T_m is the metal temperature (K); T_j is the coolant temperature (K); Q_r is the heat of reaction ($J\ h^{-1}$); Q_m is the heat transfer to metal ($J\ h^{-1}$); Q_j is the heat to coolant ($J\ h^{-1}$); C_p is the reactant specific heat (4200 $J\ kg^{-1}\ K^{-1}$); C_{pm} is the specific heat of metal (500 $J\ kg^{-1}\ K^{-1}$); C_{pj} is the specific heat of the coolant (4200 $J\ kg^{-1}\ K^{-1}$); ρ is the reactant density (800 $kg\ m^{-3}$); ρ_m is the density of the metal (8200 $kg\ m^{-3}$); ρ_j is the density of the coolant (1000 $kg\ m^{-3}$); V is the reactant volume (1.23 m^3); V_m is the volume of the metal (0.27 m^3); V_j is the volume of the coolant (0.53 m^3); ΔH_1 and ΔH_2 are the reaction enthalpy constants (-6.50 × 10^8 and -1.20 × 10^8 $J\ kmol^{-1}$, respectively); U_i is the inside heat-transfer coefficient (7.0×10^6 $J\ h^{-1}\ K^{-1}\ m^{-2}$); U_o is the outside heat-transfer coefficient (8.18×10^6 $J\ h^{-1}\ K^{-1}\ m^{-2}$); A_i is the inside heat-transfer area (5.25 m^2); and A_o is the outside heat-transfer area (5.25 m^2).

It is assumed [16] that the system is preheated to 350 K and the jacket is filled with water at 300 K. The initial conditions are: $C_a(t0) = 0.975$; $C_b(t0) = 0.025$; $C_c(t0) = 0$; $T(t0) = 350\ K$; $T_m(t0) = 373\ K$; and $T_j(t0) = 300\ K$.

III. Dynamic Optimization of the Batch Reactor

A. The FBTP

In the *FBTP*, with a specified final batch time, t_b, and dynamic model equation, $\boldsymbol{f}$, the desired product concentration, x_d, is maximized as:

$$\max_{F_j} x_d(t_b)$$

s.t.

$$\dot{\boldsymbol{x}} = \boldsymbol{f}(\boldsymbol{x}, F_j, \boldsymbol{p}), \qquad \boldsymbol{x}(t_0) = \boldsymbol{x_0} \quad (12a)$$

$$0 < F_j(t) < F_U \quad (12b)$$

$$T(t) < T_U \quad (12c)$$

$$T(t_b) < T_f \quad (12d)$$

$$x_W(t_b) < x_{Wf} \quad (12e)$$

where $\boldsymbol{x}(t)$ is an n-dimensional state vector; $\boldsymbol{p}$ is a parameter vector; F_j is the coolant flow; F_U is the upper bound of the coolant flow; x_W is the waste; x_{Wf} is the end-point concentration for the waste; T_U is the upper bound of the reactor temperature; T_f is the end-point temperature of the reactor; and t_0 is the initial time.

For the process described in Section II, $\boldsymbol{x} = [C_a,\ C_b,\ C_c,\ T,\ T_m,\ T_j]$; $x_d = C_b$; and $x_w = C_c$.

B. The MBTP

In the *MBTP*, the optimization objective is to minimize the batch time required to satisfy some performance specifications such as to obtain a required end-point concentration value, x_f, for x_d, by manipulating the coolant flow rate as:

$$\min_{F_j} t_b$$

s.t.

$$\dot{\boldsymbol{x}} = \boldsymbol{f}(\boldsymbol{x}, F_j, \boldsymbol{p}), \qquad \boldsymbol{x}(t_0) = \boldsymbol{x_0} \quad (13a)$$

$$0 < F_j(t) < F_U \quad (13b)$$

$$T(t) < T_U \quad (13c)$$

$$T(t_b) < T_f \quad (13d)$$

$$x_W(t_b) < x_{Wf} \quad (13e)$$

$$x_d(t_b) = x_f \quad (13f)$$

For the process described in Section II, $x_f = C_{bf}$.

In a time optimal problem it is in the interest of the chemical process industry to shorten the batch time and to drive the processes closer to their real constraints.

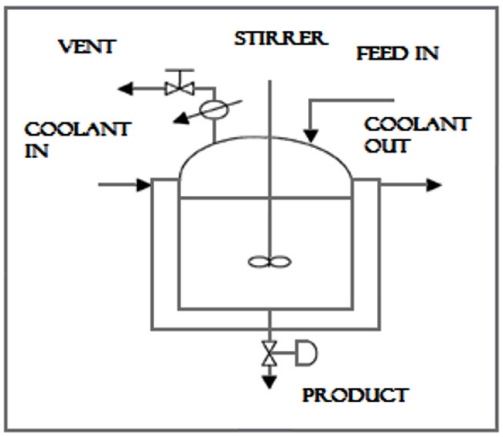

Figure 1. A jacketed batch reactor.

C. Method of Simultaneous Optimization

The main characteristic of the simultaneous approach is the fact that the optimization is carried out in the space of discretized inputs and states. Here, the inputs and the states are parameterized using a finite number of decision variables. The differential equations are discretized via orthogonal collocation [9]; therefore, the differential equations are satisfied only at a finite number of time

instants. These steps lead to a standard nonlinear programming problem (*NLP*) which is solved using a method such as the successive quadratic programming (*SQP*). Thus, in general, the dynamic equations and the discretized constraints are satisfied at the solution of the optimization problem only.

IV. Open-Loop Reactor Operation

In the open-loop reactor operation the optimization is merely carried out at the start of the batch time. Then the control input computed by the optimization algorithm is applied to the process for the duration of the batch time. No process measurement is performed to modify the control input during the batch time.

In the simultaneous optimization approach described in Subsection III.C, the optimization is carried out in the space of discretized variables. This means that the discretized constraints are in general satisfied at the solution of the optimization problem only. Therefore, the shape of the waveform connecting the computed discrete points of the input trajectory may lead to different process responses. In this project, the control input applied to the process can either be in the form of a rectangular pulse or a multi-stage staircase waveform. The durations of these two waveforms extend from any two consecutive points (boundary or collocation) on the finite elements. For the multi-stage staircase input, these durations are divided into *Nsteps* number of equal steps. The manipulating input is assumed to be constant during each step.

Due to the lack of process measurements during the batch time, the process response is highly affected by the disturbances and model mismatch.

V. Closed-Loop Reactor Operation

A. Closed-Loop Method based on the VNFE (CLVNFE)

If rapid response to a disturbance is needed, the optimal profiles must be re-evaluated online. The online optimization, *CLVNFE,* employs a modification of the scheme known as the shrinking horizon *NMPC* described in Diehl et al. [10], Eaton & Rawlings [11], Liotta et al. [12], Soni & Parker [13], and Thomas et al. [14]. In this method, the batch time is divided into a number of equal length intervals with one finite element per interval. The number of these intervals, n_i, is the initial prediction horizon (*PH*) and control horizon (*CH*) of an *NMPC* scheme. The first optimization run (*OR*), executed at time $t = 0$, employs all *PH* elements to compute the optimal input trajectory. The computed control inputs of the first element are then applied to the process. Process measurements, as explained in Subsection VI.C.i, are taken at the end of the first element and at this point in time a new *OR* is then carried out with $PH = CH = n_i - 1$. The measurements are used as the initial vector $\boldsymbol{x_0}$ for the new *OR*. This process is subsequently repeated until the final *OR* which is carried out with $PH = CH = 1$. The size of the horizon during the online optimization of the batch process is decremented by one at each *OR*. Here, the number of measurements $N_{meas} = n_i - 1$. These measurements are employed in the optimization algorithm to compensate for the effects of process disturbances. Between any two *OR*s the process is run in open loop.

As in the open-loop operation, the control input applied to the process can either be in the form of a rectangular pulse or a multi-stage staircase waveform extending between any two consecutive collocation points (or a boundary point and a collocation point) of the finite elements. For further clarification of the method please read the numerical example explained in the first paragraph of Subsection VI.C.i.

B. Closed-Loop Method based on the VNCP (CLVNCP)

Due to disturbances during operations, there is a risk of generating substandard batches where the product or safety conditions are not met and the path or end-point constraints are violated. Process data are obtained online, by measuring one or more process variables, and used to establish an improved operating policy for the rest of the batch time. In the *CLVNFE* described above, the process is run in open loop during each interval. Therefore, to increase the accuracy of the computed optimal points, it is required to increase the number of intervals in the batch time. However, we will demonstrate in Section VI that any increase in the number of intervals increases the computational effort. Here in the *CLVNCP*, we attempted to formulate an optimization scheme based on a fixed and small number of intervals (two for example) per batch time. We assume an initial number of collocation points on each interval and reduce the number of collocation points, in place of the number of intervals, as the end of the batch time is approached. The number of collocation points on each finite element, n_{col}, is decremented as the experiment is moved forward more than a threshold time gap, t_g, equal to n_i times the average collocation time, t_{ac}, defined as:

$$t_{ac} = \frac{t_b}{n_i(n_{col}+1)}. \tag{14}$$

The computed control input applied to the process can either be in the form of a rectangular pulse or a multi-stage staircase waveform. The duration of the control waveform, t_{cw}, applied to the process extends from the staring boundary of the foremost finite element (in each *OR*) to the first collocation point on this element. The horizon chosen for the next *OR* extends from this collocation point to the end of the batch time. Process measurements, as explained in Subsection VI.C.ii, are acquired at the end of each t_{cw}. The measurements are used as the initial vector $\boldsymbol{x_0}$ for the subsequent *OR*. The algorithm terminates after the computation and consequent application of the manipulating input (to the process) corresponding to the *OR* when its horizon reaches to a value less than t_g. To observe additional clarifications of this approach, please refer to the numerical examples given in Subsection VI.C.ii.

VI. Results

A. Optimization and Open-Loop Results for the FBTP

In the *FBTP*, the objective is to maximize the conversion of the desired product *B*. In the reaction, an end-point constraint for the reactant temperature ($T \leq 320$ *K*) is imposed to guarantee that the products are at or below certain desired temperature. The total batch time is fixed and equal to 4 *h* and the number of finite elements, n_i, is 2. Coolant flow is bounded between 0 m^3/h (valve fully closed) and 9 m^3/h (valve fully open). The end-point inequality constraint for the waste (product *C*) is set to 0.10. The reactor temperature must not exceed 360 *K* at any time (path constraint). Number of collocation points on each finite elements of *u*, *Ncolu*, and number of collocation points on each finite element of ***x***, *Ncolx*, both are equal to five.

Fig. 2 shows the concentration profile of the raw material C_a, the concentration profile of the desired product C_b, the concentration profile of the by-product C_c, the reactor temperature profile T and the optimal coolant profile F_j. From this figure, the value of the achieved conversion to the desired product $C_b(t_b) = 0.637$, the end-point concentration for the waste $C_c(t_b) = 0.098$ and the end-point reactor temperature $T(t_b) = 320$ K. These results clearly show that the two end-point constraints and the path constraint are satisfied.

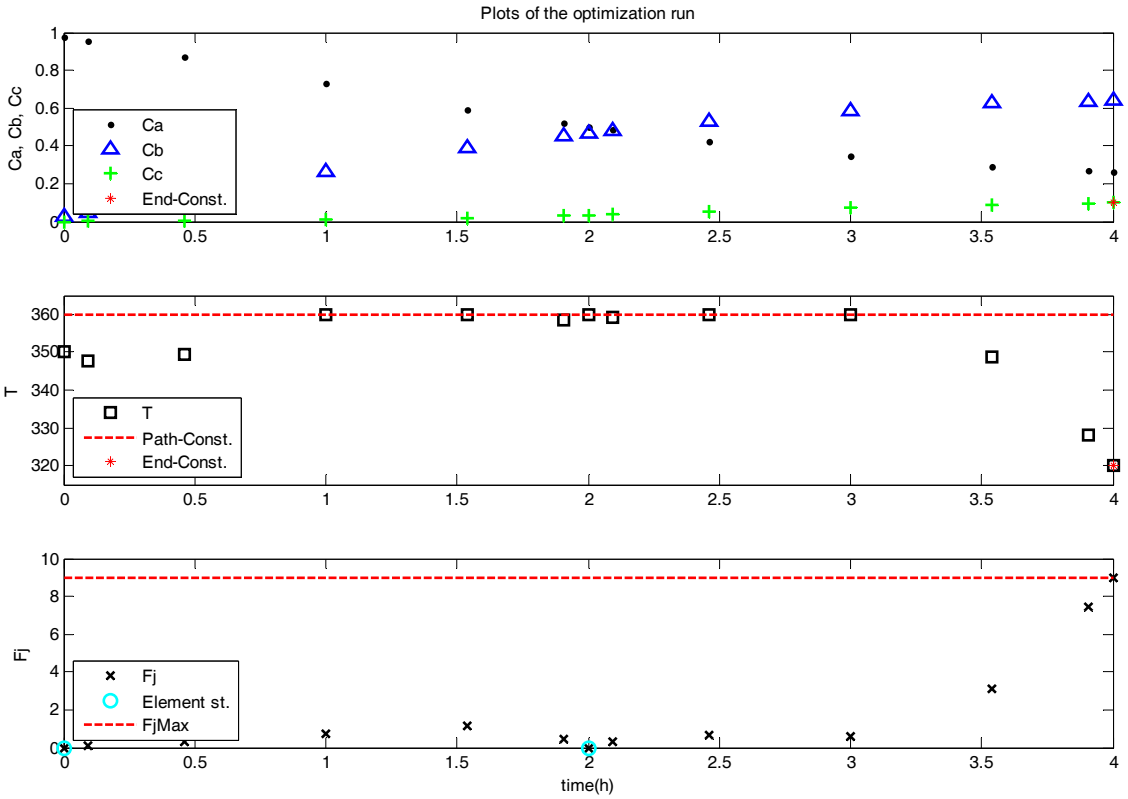

Figure 2. The optimization results for the reactor model (*FBTP*, *Ncolu* = 5, *Ncolx* = 5, $n_i = 2$).

The computed optimal control input in Fig. 2 is applied to the process. The control input applied to the process is taken to be in the form of a rectangular pulse. The duration of the pulse extends from any two consecutive optimal points (boundary or collocation) on the finite elements. Fig. 3 shows the output profiles for C_a, C_b and C_c; the profiles for the output T and input F_j. From this figure the values for $C_b(t_b) = 0.663$, $C_c(t_b)=0.164$ and $T(t_b) = 338.6$. These results demonstrate that contrary to the results shown in Fig. 2, the end-point constraints and the path constraint are violated. The violations are due to the inherent disadvantage of the simultaneous optimization method (Subsection III.C) used to determine the profiles of Fig. 2. In this and the following experiments, the path violation error is integrated to obtain the figure *I_Err* which is used to quantify this violation. For the rectangular control input used in this experiment *I_Err* = 24.27. In this case, the increase in the product yield is due to the reactor temperature violation of the path constraint.

In the manipulating input profiles of Figs. 2-13, the real locations of the collocation points within the elements are shown. In Figs. 2 and 7, the computed input profiles are theoretical and are not actually applied to the process. In Figs. 3 and 8 the level of manipulating input between any two consecutive points remains constant; and in Figs. 4-6 and 9-13, the shape of a manipulating input between any two consecutive points is in the form of a multi-level staircase as explained in Section IV.

In Fig. 4, the control input applied to the process is taken to be in the form of a staircase waveform extending between any two consecutive optimal points. The *Nsteps* parameter defined in Section IV is equal to three. Fig. 4 shows the process outputs and input profiles. From this figure the values for $C_b(t_b)$ =0. 646, $C_c(t_b) = 0.11$, $T(t_b)$= 323.3 and *I_Err* = 5.163. These results show that the staircase control input improved the performance of the reactor when compared against the rectangular input used in Fig. 3; however, all constraints are still being violated.

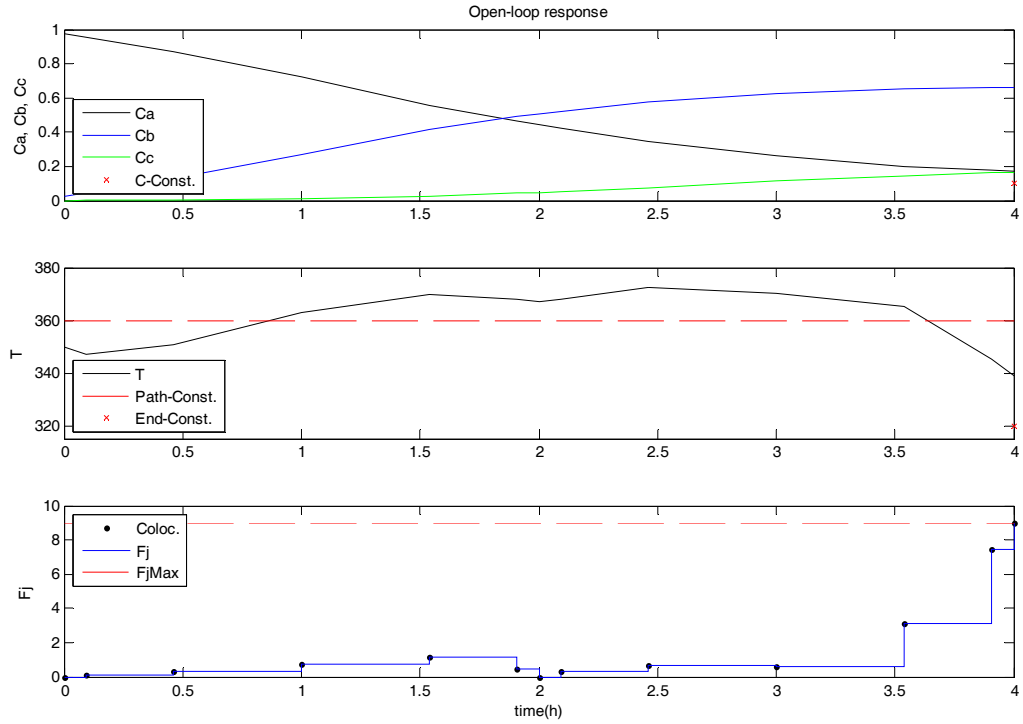

Figure 3. Open-loop operation of the reactor (*FBTP*, *Ncolu* = 5, *Ncolx* = 5, n_i = 2, rectangular control input).

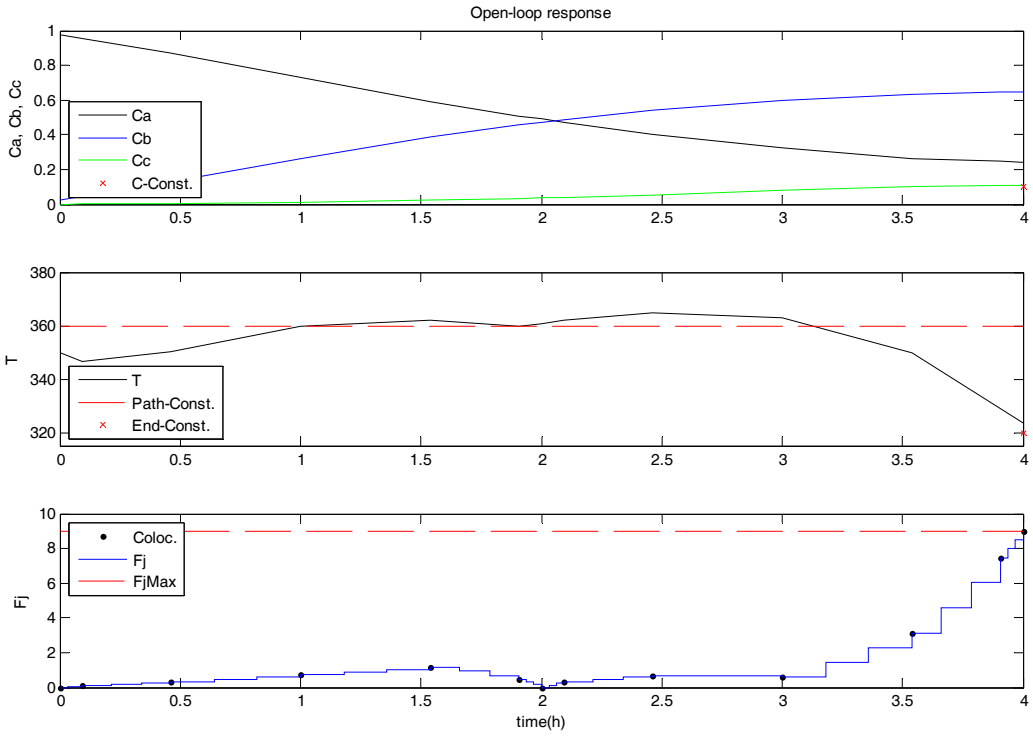

Figure 4. Open-loop operation of the reactor (*FBTP*, *Ncolu* = 5, *Ncolx* = 5, n_i = 2, staircase control input, *Nsteps* = 3).

In the next experiment, the *Nsteps parameter is* taken to be equal to five and the above experiment is repeated. Fig. 5 shows the process outputs and input profiles. From this figure the values for $C_b(t_b)$ = 0.624, $C_c(t_b)$ = 0.086, $T(t_b)$= 317.2 *K* and *I_Err* = 0.03. These results show that the end-point constraints are satisfied and *I_Err*, when compared against the previous experiment, is drastically reduced.

The control input shown in Fig. 5 is applied to the process. However, at time t = 0.9 h the process is subjected to a disturbance in the form of 65% reduction in *Ui*. Fig. 6 shows the output and input profiles. From this figure the values for $C_b(t_b)$ =0. 658, $C_c(t_b)$ = 0.140, $T(t_b)$ = 331.4 K and *I_Err* = 16.3. These results indicate that due to the process-model mismatch the end-point constraints and the path constraint are not satisfied.

B. Optimization and Open-Loop Results for the MBTP

In a time-optimal problem the objective is the minimization of the final batch time. The net conversion to the desired product is given. Here, we assumed C_{bf} = 0.6, therefore, the end-point equality constraint for the product concentration is set to 0.6. The following *MBTP* experiment employs the two terminal constraints, the path constraint, bounds, number of finite elements and number of collocation points used in the previous *FBTP* experiments. However, the *MBTP* optimizes the control variable in conjunction with the batch time.

Fig. 7 shows the states for the concentrations and the reactor temperature generated by the optimizer. From this figure the values for $C_b(t_b)$ =0.6, $C_c(t_b)$ = 0.075, $T(t_b)$ = 320 K. The optimum batch time is computed to be equal to t_{op} = 3.406 h. The user is required to specify an initial estimate for the optimum batch time. This value is set to 1.8 h in our experiment. Similar to the results shown in Fig. 2, these results show that the two end-point constraints and the path constraint are satisfied.

Two additional *MBTP* experiments are performed using staircase control inputs with N_{steps} = 1 and 3. In each experiment the computed optimal control input in Fig. 7 is applied to the process. Results similar to Figs. 3 and 4 demonstrating violations of the constraints are obtained. Then an experiment, using a staircase control input with *Nsteps* = 5, is carried out. No disturbance is applied in this case. Fig. 8 shows the input and output profiles. From this figure, the values for $C_b(t_b)$ =0.581, $C_c(t_b)$ = 0.064, $T(t_b)$ = 317.6 K and *I_Err* = 0. All the terminal constraints, the path constraint and bounds are satisfied.

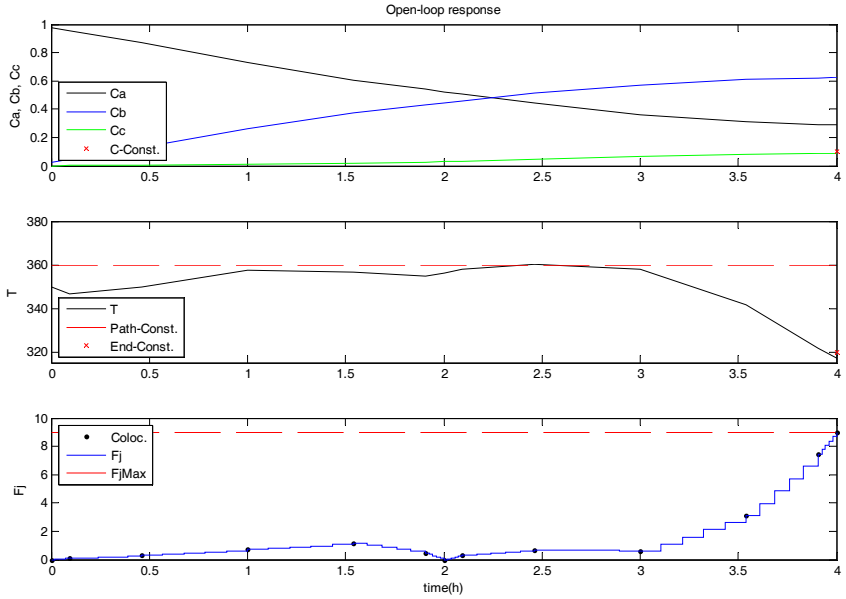

Figure 5. Open-loop operation of the reactor (*FBTP*, *Ncolu* = 5, *Ncolx* = 5, n_i = 2, staircase control input, N_{steps} = 5).

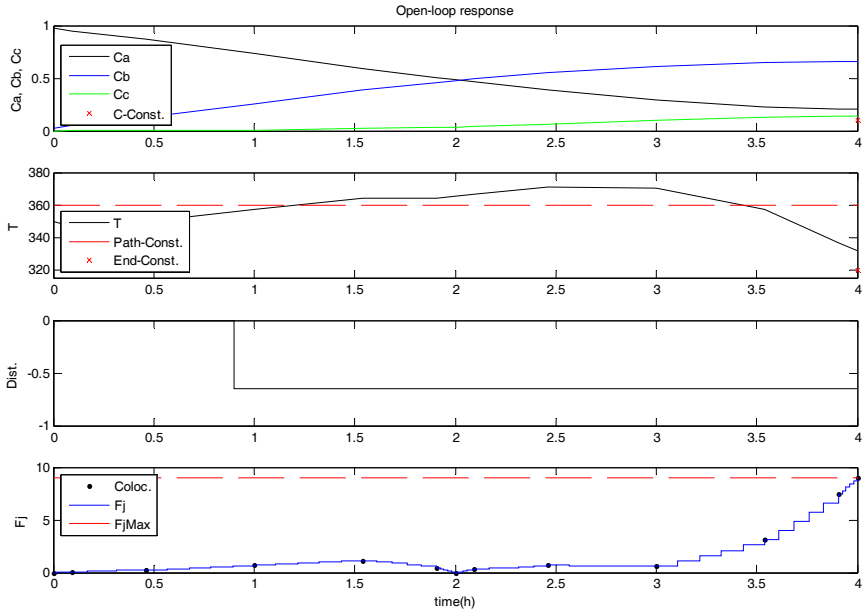

Figure 6. Pen-loop operation of the reactor with disturbance (*FBTP*, *Ncolu* = 5, *Ncolx* = 5, n_i = 2, staircase control input, *Nsteps* = 5).

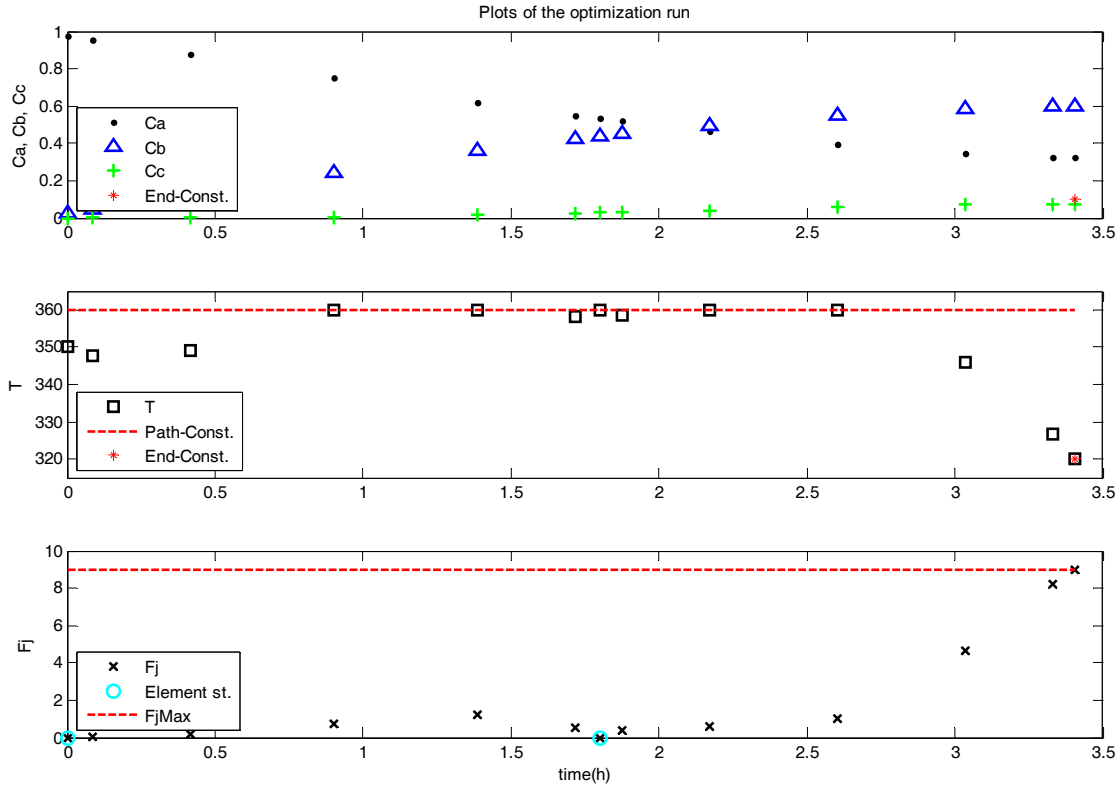

Figure 7. The optimization results for the reactor model (*MBTP*, *Ncolu* = 5, *Ncolx* = 5, n_i = 2).

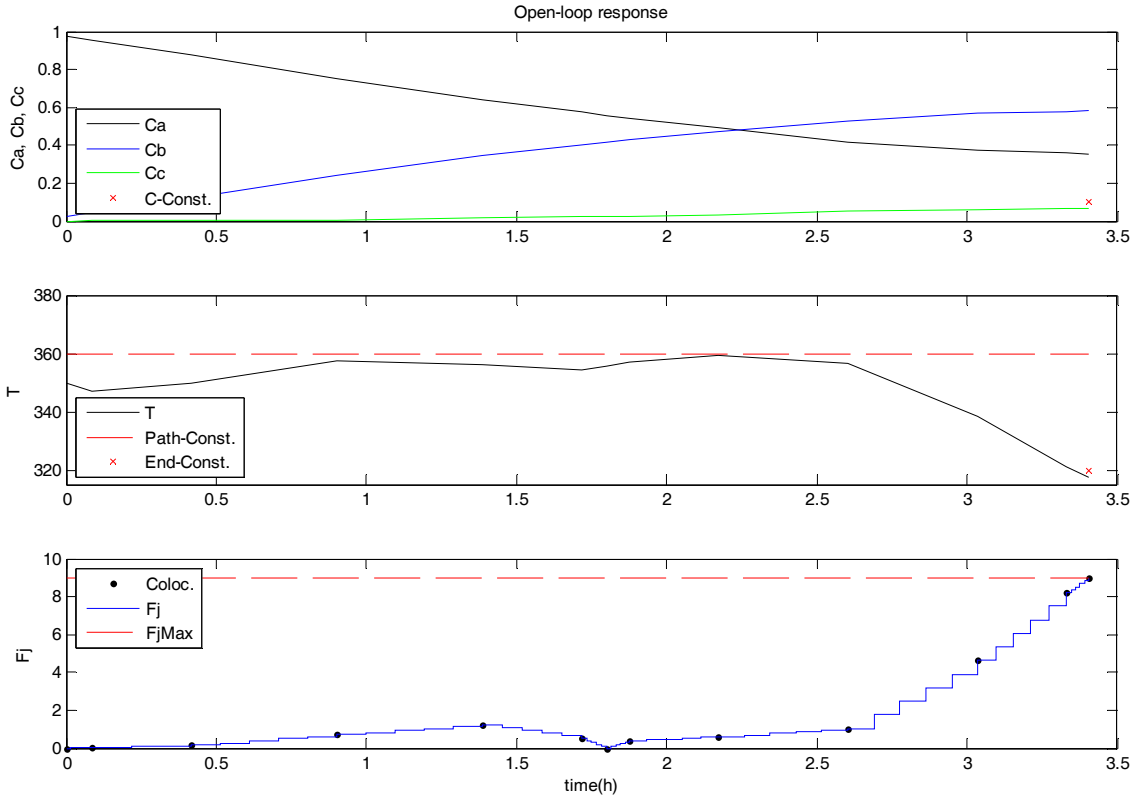

Figure 8. Open-loop operation of the reactor (*MBTP*, *Ncolu* = 5, *Ncolx* = 5, n_i = 2, staircase control input, *Nsteps* = 5).

A disturbance as defined in Fig. 6 is then applied to the process. Fig. 9 shows the resulting input and output profiles. From this figure the values for $C_b(t_b)$ =0.627, $C_c(t_b)$ = 0.1, $T(t_b)$ = 333 *K* and *I_Err* = 9.85. It can be seem that due to the process-model mismatch the terminal and path constraints on temperature are not satisfied. A summary of the results of the experiments performed so far is given in Table I.

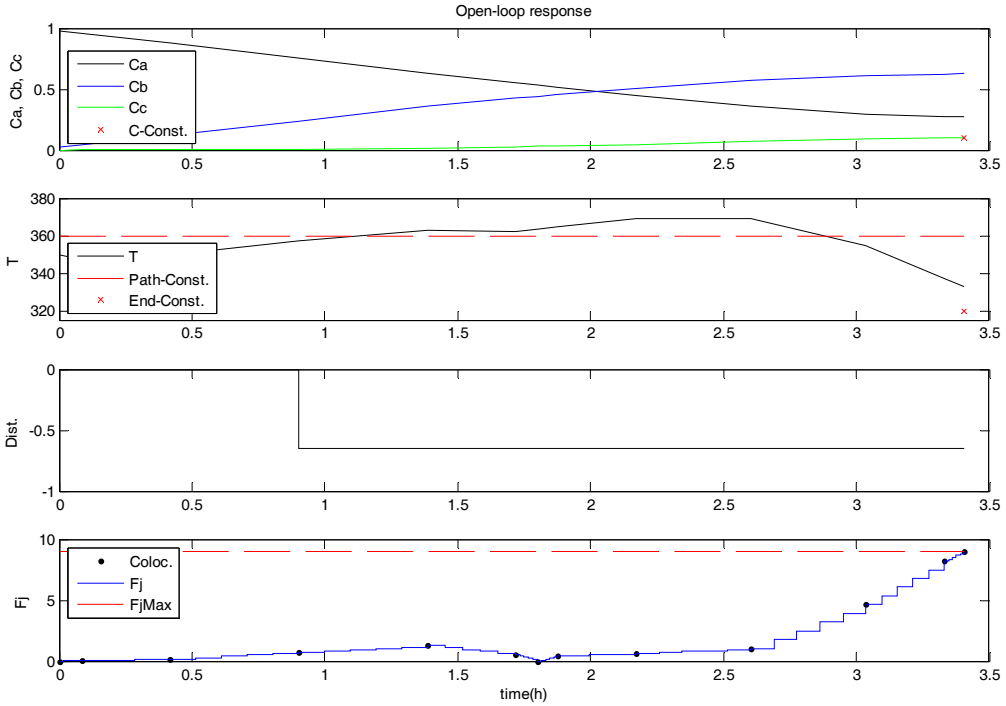

Figure 9. Open-loop operation of the reactor with disturbance (*MBTP*, *Ncolu* = 5, *Ncolx* = 5, n_i = 2, staircase control input, *Nsteps* = 5).

TABLE I. OPTIMIZATION AND OPEN-LOOP RESULTS (N_I = 2)

Problem	*Dist.*	t_b(h)	*Nsteps*	$C_b(t_b)$	$C_c(t_b)$	$T(t_b)$ (*K*)	*I_Err*	*Fig.*
FBTP	0%	4	-	0.637	0.098	320	0	2
FBTP	0%	4	1	0.663	0.164	338.6	24.27	3
FBTP	0%	4	3	0.646	0.11	323.3	5.163	4
FBTP	0%	4	5	0.624	0.086	317.2	0.03	5
FBTP	- 65%	4	5	0.658	0.140	331.4	16.3	6
MBTP	0%	3.406	-	0.6	0.075	320	0	7
MBTP	0%	3.406	5	0.581	0.064	317.6	0	8
MBTP	- 65%	3.406	5	0.627	0.1	333	9.85	9

C. Results for the Online Optimization

1) Results for the online optimization CLVNFE

If reaction to the presented disturbance in Fig. 6 (or in Fig. 9) is necessary, the optimal profiles must be re-calculated online. Here, we use the developed *CLVNFE*, as described in Subsection V.A. The batch time is divided into five identical finite elements (Ni_{max} = 5) each containing two collocation points. The *Nsteps* parameter defined in Section IV is equal to five. The optimization algorithm is invoked five times. At t = 0, the first *OR* utilizes all five finite elements as the prediction horizon and control horizon (i.e., *PH* = *CH* = 5). At $t = t_b$ /5, the second *OR* employs elements 2 to 5 (with *PH* = *CH* = 4). At $t = 2t_b$ /5, the third *OR* employs elements 3 to 5 (with *PH* = *CH* = 3). At $t = 3t_b$ /5, the fourth *OR* employs elements 4 and 5 (with *PH* = *CH* = 3). Finally, at $t = 4t_b$ /5 the fifth *OR* employs element 4 (with *PH* = *CH* = 1). In addition, process measurements corresponding to the differential variables are taken at $t = t_b/5$, $2t_b/5$, $3t_b/5$ and $4t_b/5$. Fig. 10 shows the output and input profiles. From this figure the values for $C_b(t_b) = 0.574$, $C_c(t_b) = 0.060$, $T(t_b)$ = 307.6 *K*, and *I_Err* = 5.52. The computational effort of the whole batch process algorithm t_e = 27.2 *s*. The system used to execute the codes in this paper is a microcomputer with *AMD* 3.0+ *GHz CPU*, 512*M* bytes *RAM* and 512*k* bytes cache memory. These results indicate that by feeding back the measurements at the sampling points, the end-point constraints are satisfied. Also, for the path constraint, the value of *I_Err* = 5.52 is smaller than *I_Err* = 16.3 resulted in Fig. 6. In this experiment, the horizons are decremented at consecutive *OR*s in order to reduce the computational load and avoid control pulses with undersized extends being computed and then applied to the process.

To enhance the performance of the above experiment, the batch time is divided into 6 identical finite elements (Ni_{max} = 6) each containing two collocation points. The *Nsteps* parameter used in the previous experiment is decremented by one (i.e, *Nsteps* = 4) to avoid control pulses with undersized extends being applied to the process. The optimization algorithm is invoked six times. In addition, the process measurements take place at $t = t_b/6$, $t_b/3$, $t_b/2$, $2t_b/3$ and $5t_b/6$. Fig. 11. shows the resulting output and input profiles. From this figure the values for $C_b(t_b)$ =0. 538, $C_c(t_b)$ = 0.045, $T(t_b)$ = 306.2 K, *I_Err* = 2.84 and t_e = 53.5 s. These results indicate that by feeding back five sets of process measurements (N_{meas} = 5), the end-point constraints are satisfied. Also, for the path

constraint, the value of *I_Err* = 2.85 is smaller than *I_Err* = 5.52 of the previous experiment.

Employing the optimization *CLVNFE*, two more experiments are carried out using Ni_{max} = 7 and 8 (with *Nsteps* = 3 and 2, respectively). A summary of the results of the four experiments performed in this subsection is given in Table II. It can be seen that a reduction in *I_Err* is achieved at the expense of an increase in the computational effort and a decrease in the concentration of the desired product.

TABLE II. CLVNFE (*NCOL* = 2; T_B = 4 H; *DIST.* = - 65%)

Ni_{max}	*Nsteps*	N_{meas}	$C_b(t_b)$	$C_c(t_b)$	$T(t_b)$ (*K*)	t_e(*s*)	*I_Err*	*Fig.*
5	5	4	0.574	0.060	307.6	27.2	5.52	10
6	4	5	0.538	0.045	306.2	53.5	2.85	11
7	3	6	0.516	0.038	305.8	63.8	1.41	-
8	2	7	0.502	0.034	305.4	142.6	1.12	-

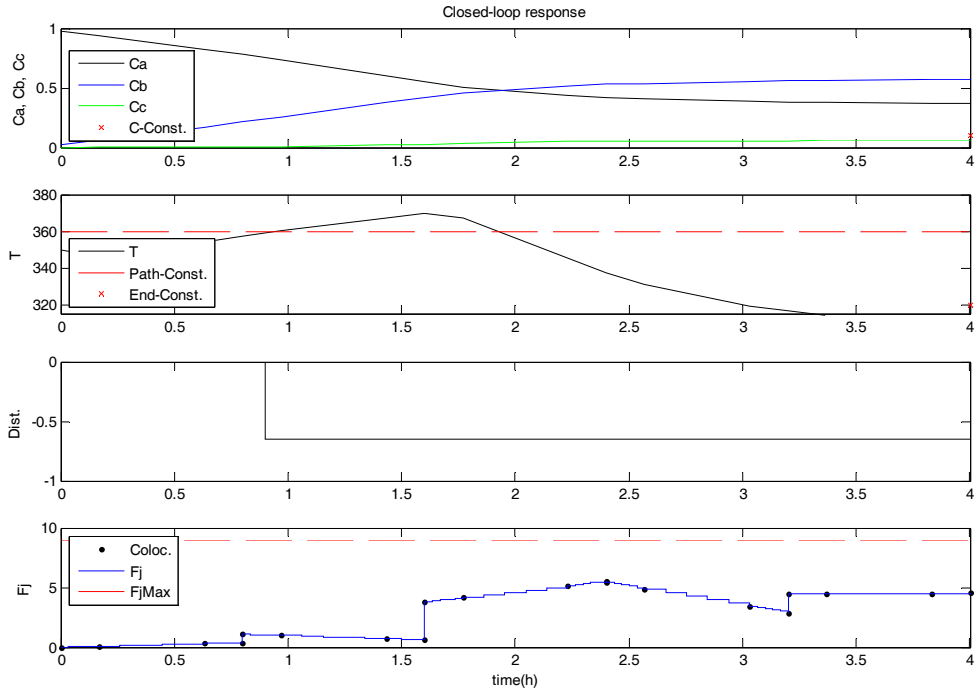

Figure 10. Closed-loop operation of the reactor using the *CLVNFE* (*FBTP*, *Ncol* = 2, Ni_{max} = 5, staircase control input, *Nsteps* = 5).

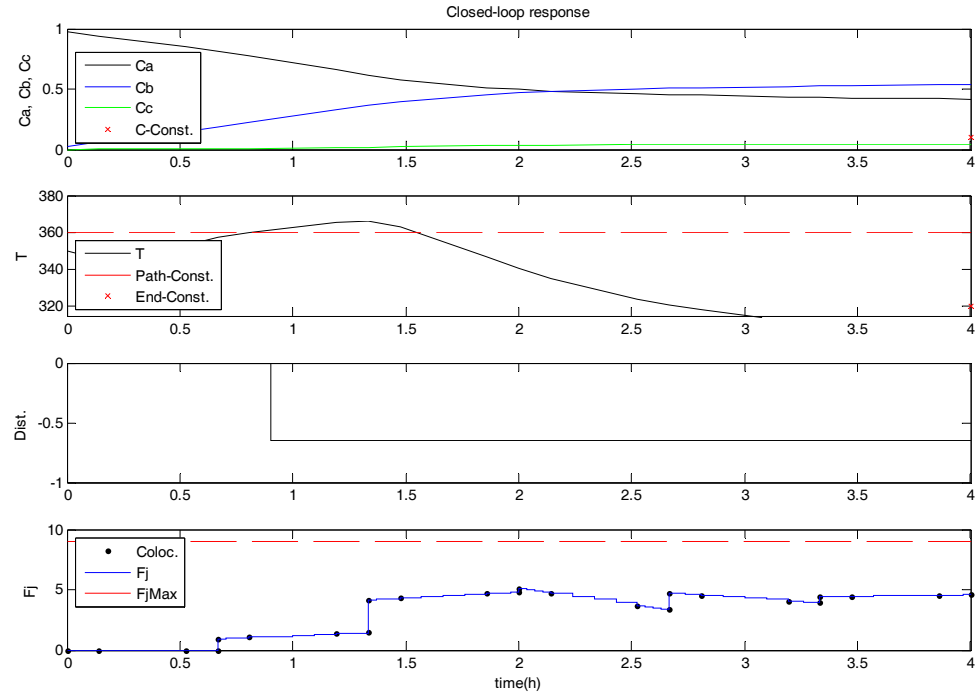

Figure 11. Closed-loop operation of the reactor using the *CLVNFE* (*FBTP*, *Ncol* = 2, Ni_{max}= 6, staircase control input, *Nsteps* = 5).

2) Results for the online optimization CLVNCP

Here, the developed *CLVNCP*, as described in Subsection V.B is used to react to the presented disturbance in Fig. 6. At this time, two finite elements each of which consisting of an initial maximum number of three collocation points on $\boldsymbol{x}$ and u, $Ncol_{max}$, are used for the entire batch time. *Nsteps* is equal to 5. The threshold time gap (defined in Subsection V.B) $t_g = n_i t_{ac}$ =1 *h*. Based on this figure, as the experiment is progressed, the number of collocation points on the finite elements is decremented to reduce the computational load and avoid control pulses with undersized lengths being computed and consequently applied to the process. Table III gives a summary of the overall optimization process throughout the batch time. The first row in this table shows the *OR* number; the second row gives the starting time of each *OR* and the data measurement times; the third row gives the horizon corresponding to each starting time in the second row; and the fourth row gives the number of collocation points of the finite elements. As shown in this table, the batch time consists of three time gaps in each of which the implemented *OR*s employ the same number of collocation points. The first time gap extends from 0 to 1.007 *h*. Four *OR*s with *Ncol* = 3 are performed in this gap. Four sets of measurements (at t = 0.225, 0.438, 0.639 and 0.828 *h*), each of which specifying the values corresponding to the differential variables, are acquired in the first time gap. Two other time gaps start at t = 1.007 and 2.085 *h*. The optimization procedure is invoked thirteen times during the batch time and requires twelve sets of process measurements (N_{meas} =12).

Fig. 12 shows the output and input profiles for this experiment. From this figure the values for $C_b(t_b)$ =0. 602, $C_c(t_b)$ = 0.071, $T(t_b)$ = 314.31 K, *I_Err* = 0.76 and t_e = 24 s. These results indicate that by feeding back twelve sets of process measurements, the end-point constraints are satisfied. Also, for the path constraint, the value of *I_Err* = 0.76 is smaller than *I_Err* = 5.52 resulted in Fig. 10 and *I_Err* = 2.84 resulted in Fig. 11. In addition, the computational load t_e = 24 s is smaller than t_e = 27.2 s required in Fig. 10 and t_e = 53.5 s required in Fig. 11.

TABLE III. OVERALL OPTIMIZATION PROCESS SHOWN IN FIG. 12 ($NCOL_{MAX}$ = 3; T_B = 4 *H*; N_I = 2; *NSTEPS* = 5; DIST. = - 65%)

OR	1	2	3	4	5	6	7	8	9	10	11	12	13
t (hr)	0	0.225	0.438	0.639	0.828	1.007	1.323	1.606	1.859	2.085	2.564	2.923	3.192
Horizon (hr)	4	3.775	3.562	3.361	3.172	2.993	2.677	2.394	2.141	1.915	1.436	1.077	0.808
Ncol	3	3	3	3	3	2	2	2	2	1	1	1	1

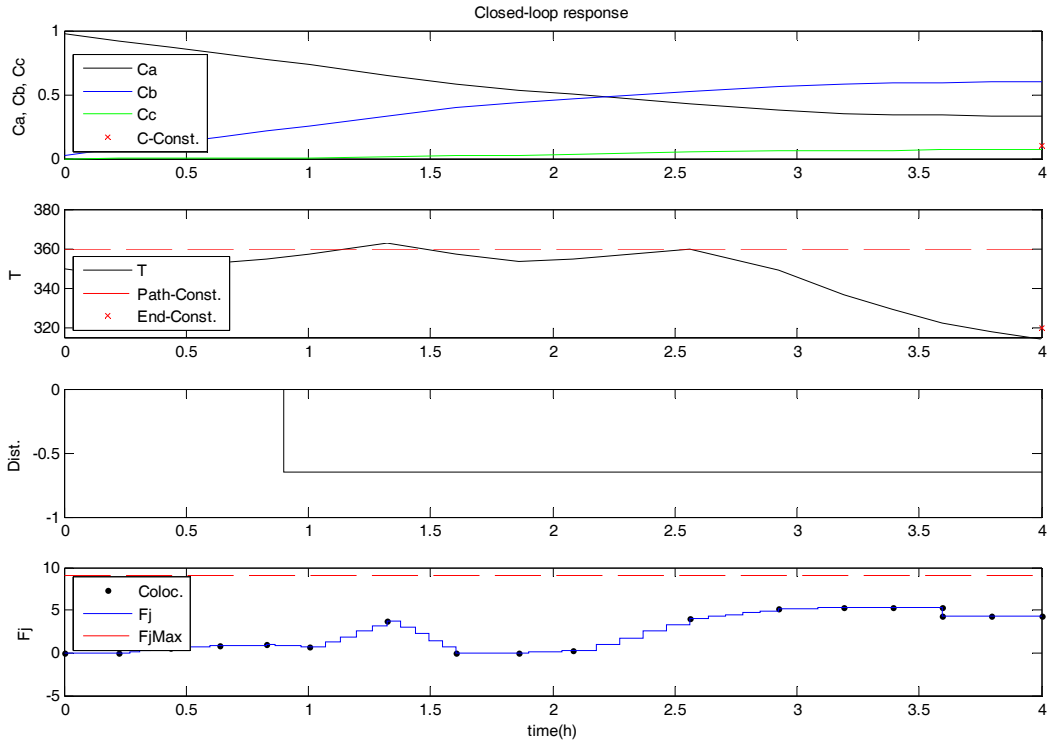

Figure 12. Closed-loop operation of the reactor using the *CLVNCP* (*FBTP*, $Ncol_{max}$ = 5, $Ncol_{min}$ = 1, n_i = 2, staircase control input, *Nsteps* = 5).

Now, we take $Ncol_{max}$ = 4 (*Nsteps* = 4) and repeat the above experiment. Fig. 13 shows the resulting output and input profiles. From this figure the values for $C_b(t_b)$ =0. 604, $C_c(t_b)$ = 0.072, $T(t_b)$ = 314.8, *I_Err* = 0.73 and t_e = 50 *s*. The performance improvement when compared against the previous run is achieved at the expense of an increase in the computational load.

Employing the optimization *CLVNCP*, two more experiments are carried out with $Ncol_{max}$ = 5 and 6 (the corresponding *Nsteps* = 3 and 2, respectively). A summary of the results of the four experiments performed in this subsection is given in Table IV. It can be seen that a reduction in *I_Err* is achieved at the expense of an increase in the computational effort. However, unlike the

results obtained for the *CLVNFE*, the concentration of the desired product increases as $Ncol_{max}$ is increased. For comparable computational loads: (i) *I_Err* has a lower magnitude in the *CLVNCP* than the corresponding value in the *CLVNFE*; and (ii) the desired product concentration in the *CLVNCP* is higher than the product concentration in the *CLVNFE*.

In all the online experiments, explained in the current subsection, the *FBTP* trial is assumed. Similar procedures can be carried out for the system if the *MBTP* testing is required.

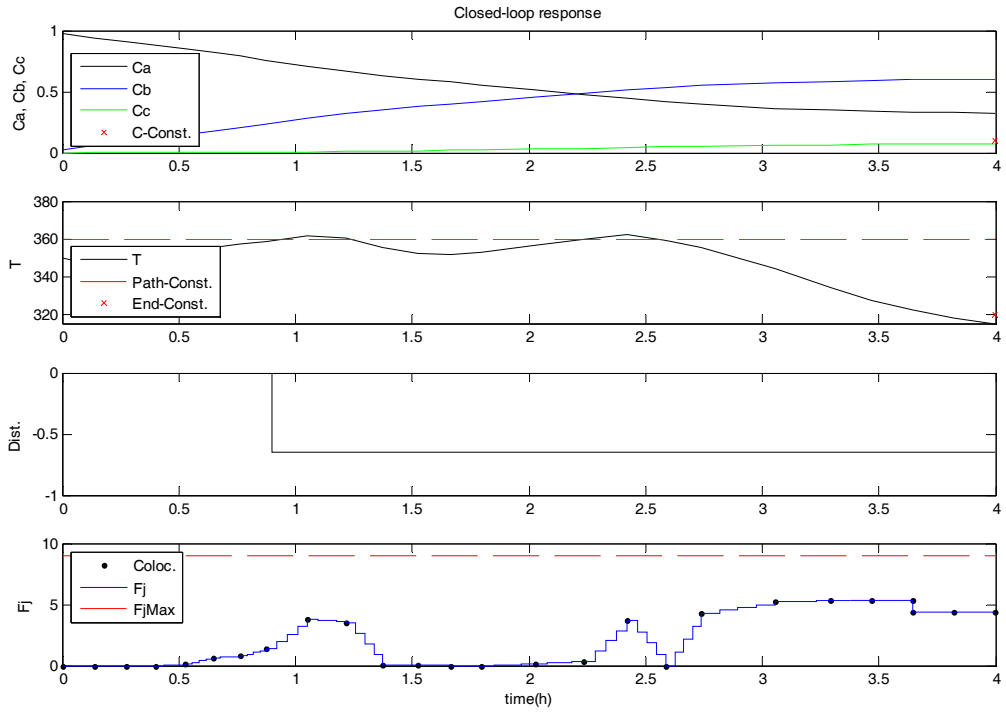

Figure 13. Closed-loop operation of the reactor using the *CLVNCP* (*FBTP*, $Ncol_{max}$ = 6, $Ncol_{min}$ = 1, n_i = 2, staircase control input, *Nsteps* = 4).

TABLE IV: *CLVNCP* (N_i = 2; T_B = 4 *H; DIST.* = - 65%)

$Ncol_{max}$	*Nsteps*	N_{meas}	t_g (h)	$C_b(t_b)$	$C_c(t_b)$	$T(t_b)$ (*K*)	t_e (s)	*I_Err*	Fig.
3	5	12	1	0.602	0.071	314.3	24	0.76	12
4	4	20	0.8	0.604	0.072	314.8	50	0.73	13
5	3	28	0.667	0.609	0.074	316.6	92	0.67	-
6	2	38	0.571	0.619	0.081	318.5	274	0.34	-

VII. Conclusions

An appropriate input wave shaping combined with simultaneous optimization method improved the system operation when the batch reactor is operated in open loop. In the closed-loop operation, the online optimization *CLVNCP* developed in this article when compared against the *CLVNFE*: (i) imposes a lower computational effort to achieve comparable levels of *I_Err* in the two methods; (ii) produces a higher level of the desired product concentration for comparable levels of the path violation errors *I_Err* in the two methods; and (iii) increases the level of the desired product concentration as the optimization parameters are adjusted to reduce *I_Err*. This action reduces the product yield in the *CLVNFE*.

Nomenclature

A_i	inside heat-exchange area (m^2)
A_o	outside heat-exchange area (m^2)
C_i	concentration ratio of the component i ($kmolm^{-3}$)
C_p	specific heat of reactant ($J\,kg^{-1}\,K^{-1}$)
C_{pm}	specific heat of metal ($J\,kg^{-1}\,K^{-1}$)
C_{pj}	specific heat of cooling liquid ($J\,kg^{-1}\,K^{-1}$)
CH	control horizon
DAE	differential-algebraic equation
E_i	activation energy for reaction *i* ($J\,kmol^{-1}$)
FBTP	fixed batch-time problem
F_j	cooling liquid flow rate ($m^3\,h^{-1}$)
I_Err	integral of path violation error
ΔH_i	enthalpy of reaction for reaction *i* ($J\,kmol^{-1}$)
$k_{i,0}$	pre-exponential constant (h^{-1})
k_i	reaction rate constant for reaction *i* (h^{-1})
MBTP	minimum batch-time problem
CLVNCP	closed-loop method based on the *VNCP*
CLVNFE	closed-loop method based on the *VNFE*
n_i	number of finite elements
Ncol	number of collocation points on *u* and ***x***
Ncolu	number of collocation points on each finite element of *u*
Ncolx	number of collocation points on each finite element of ***x***
NLP	nonlinear problem
N_{meas}	number of measurements
NMPC	nonlinear model predictive control
Nsteps	number of steps of the staircase

OR	optimization run
$\boldsymbol{p}$	parameter vector
PH	prediction horizon
Q_j	amount of heat transferred to cooling liquid ($J\ h^{-1}$)
Q_m	amount of heat transferred to metal ($J\ h^{-1}$)
Q_r	amount of heat generated by the reaction ($J\ h^{-1}$)
R	universal gas constant $J\ kmol^{-1}\ K^{-1}$
SQP	successive quadratic programming
t	time (h)
t_b	batch time (h)
t_{ac}	average collocation time (h)
t_{cw}	duration of control waveform (h)
t_e	computational effort
t_g	threshold time gap
t_{op}	optimal batch time (h)
T	temperature of reaction mixture (K)
T_j	temperature of cooling liquid (K)
T_{j0}	inlet temperature of cooling liquid (K)
T_m	temperature of the reactor metal (K)
U_i	inside heat-transfer coefficient ($J\ h^{-1}\ K^{-1}\ m^{-2}$)
U_o	outside heat-transfer coefficient ($J\ h^{-1}\ K^{-1}\ m^{-2}$)
V	volume of reactor contents (m^3)
V_j	volume of cooling liquid (m^3)
V_m	volume of reactor metal (m^3)
$VNFE$	variable number of finite elements
$VNCP$	variable number of collocation points
$\boldsymbol{x}$	vector of variables

Greak letters

ρ_m	density of metal (kg m^{-3})
ρ_j	density of cooling liquid (kg m^{-3})

REFERENCES

[1] B. Srinivasan, S. Palanki, and D. Bonvin, "Dynamic optimization of batch process, I. characterization of nominal solution," *Computers Chem. Engng,* vol. 27, no. 1, pp. 1-26, January 2003.

[2] C. Loeblein, J. D. Perkins, B. Srinivasan, and D. Bonvin, "Performance analysis of online batch optimization system," *Computers Chem. Engng,* vol. 21, pp. S867-S872, May 1997.

[3] D. Ruppen, C. Benthack, and D. Bonvin, "Optimization of batch reactor operation under parameter uncertainty-computational aspects," *J. of Proc. Cont.,* vol. 5, no. 4, pp. 235-240, November 1995.

[4] M. Ropotar and Z. Kravanja, "Development of a mathematical model for the dynamic optimization of batch reactors, and MINLP synthesis of plug-flow reactors in complex networks," *Acta Chim. Slov.,* vol. 54, no. 4, pp. 700-712, April 2007.

[5] O. Abel and W. Marquardt, "Scenario-integrated online optimization of batch reactors," *Jounal of Process Control,* vol. 13, no. 8, pp. 703-715, December 2003.

[6] T. Ishikawa, Y. Natori, L. Liberis, and C. C. Pantelides, "Modelling and optimization of an industerial batch process for the production of dioctyl phthalate," *Computers Chem. Engng,* vol. 21, pp. S1239-S1244, May 1997.

[7] R. B. Zapata, A. L. Villa, C. M. de Correa, L. Ricardez-Sandoval, and A. Elkamel, "Dynamic modeling and optimization of a batch reactor for limonene epoxidation," *Ind. Eng. Chem. Res.*, vol. 49, no.18, pp. 8369–8378, July 2010.

[8] L. Niu and D. Yang, "Dynamic simulation and optimization for batch reactor control profiles," in *Proc. SPIE, Fifth International Conference on Machine Vision: Algorithms, Pattern Recognition, and Basic Technologies*, Wuhan, China, vol. 8784, 20-21 October 2012.

[9] J. E. Cuthrell and L. T. Biegler, "Simultaneous optimization and solution methods for batch reactor control profiles," *Computers Chem. Engng*, vol. 13, no. 1-2, pp. 49-62, January-February 1989.

[10] M. Diehl, H. G. Bock, and J. P. Schlöder, "A real-time iteration scheme for nonlinear optimization in optimal feedback control," *SIAM J. Control and Optim.,* vol. 43, no. 5, pp. 1714-1736, September 2005.

[11] J. W. Eaton and J. B. Rawlings, "Feedback control of chemical processes using on-line optimization techniques," *Computers Chem. Engng,* vol. 14, no. 4-5, pp. 469-479, April-May 1990.

[12] V. Liotta, C. Georgakis, and M. S. El-Aasser, "Real-time estimation and control of particle size in semi-batch emulsion polymerization," in *Proc. American Control Conference, Albuquerque, NM*, vol. 2, 4-6 June 1997, pp. 1172-1176.

[13] A. S. Soni and R. S. Parker, "Closed-loop control of fed-batch bioreactors: A shrinking-horizon approach," *Industrial and Engineering Chemistry Research,* vol. 43, no. 13, pp. 3381-3393, May 2004.

[14] M. M. Thomas, J. L. Kardos, and B. Joseph, "Shrinking horizon model predictive control applied to autoclave curing of composite laminate materials," in *Proc. American Control Conference, Baltimore, Maryland*, vol. 1, 29 June-1 July 1994, pp. 505-509.

[15] M. A. Hosen, M. A. Hussain, A. Khosravi, D. Creighton, and S. Nahavandi, "Investigation of process dynamics and control of polystyrene batch reactor using hybrid model," in *Proc. World Congress on Engineering and Computer Science*, *San Francisco, USA,* vol. 2, 24-26 October 2012, pp. 765-769.

[16] N. Aziz and I. M. Mujtaba, "Optimal operation policies in batch reactors," *Chemical Engineering Journal*, vol. 85, no. 2-3, pp. 313-325, January 2002.

